Adsorption Behavior of an Adamantane Derivative on Metal Clusters – DFT Simulation Studies

Jamelah S. Al-Otaibi
Princess Nourah bint Abdulrahman University
Y. Sheena Mary (marysheena2018@rediffmail.com)
Thushara https://orcid.org/0000-0002-9082-3670
Y. Shyma Mary
Thushara

Research Article

Keywords: DFT, adamantane, metal cages, SERS.

Posted Date: July 30th, 2021

DOI: https://doi.org/10.21203/rs.3.rs-741843/v1

Abstract

Investigation of the adsorption properties of 3-(adamantan-1-yl)-4-phenyl-1-[(4-phenylpiperazin-yl)methyl]-1*H*-1,2,4-triazole-5(4*H*)-thione (APT) with metal clusters (mC: Ag, Au and Cu) are reported using DFT method. APT is found to form stable cluster with transition metal clusters of copper, silver and gold. The drug-cluster complexation energy is slightly more for the gold nanocluster-drug complex. Dipole moment of the drug-gold cluster is found to be higher than that of the other systems. SERS studies demonstrate improved Raman signals for multiple wavenumbers of all APT-metal cluster complexes. Different spectroscopic, chemical and electronic properties are also investigated.

Introduction

Viral diseases are deadly and one of the leading causes of human life around the world and they are increasing at an alarming rate, along with emergence of new viruses and mutations in the genomes of those that already exist [1]. Because of the scarcity of effective medications and fear of unknown, new viruses draw a lot of attention [2,3]. As a result, the development of effective antivirals that can be used against virus is critical; yet, discovery of novel viral inhibitors will be the century's challenge. Furthermore, constant antiviral pharmaceutical therapy has resulted in the formation of resistance to known inhibitors as well as changes in viruses, posing significant hurdles in the discovery of novel active and selective inhibitors. The lack of effective medicines for majority of viral illnesses, as well as the high cost of traditional antiviral therapies, necessitates the development of novel antiviral agents.

Many investigations have been conducted with triazole, which are important for the development of new medicines [4]. Triazole derivative's unusually structure and electron-rich system allow them to interact easily with a variety of receptors, resulting in a wide range of biological activities [5]. Antibacterial, antifungal and anticancer properties are only a few of the interesting pharmacological properties of adamantane derivatives [6-8]. Bioisosteric substitution of adamantane with lipophilic groups changes water solubility of epoxide hydrolase inhibitors [9]. Adamantane derivatives have been used as medicines with various biological activities [10].

Metal organic frameworks have piqued researcher's interest in recent decades due to their potential applications in a variety of domains, including medication administration and sensing [11,12].Coinage metals, Au, Ag and Cu have a wide range of physical and chemical properties and are often utilized as catalysts in the heterogeneous catalysis reactions [13]. Copper nanoparticles have gotten a lot of attention from the coinage metals community because of their in expensive price and ability to be used as large scale industrial catalyst [14]. Biomolecule interactions with nanostructures are a popular issue in biological applications [15]. Nanoparticles differ from their bulk counterparts in a number of ways. The size dependent features of nanomaterials give up new opportunities in a range of sectors. Gold nanoparticles for example are very popular substance due to their numerous applications [16]. Silver and gold nanoparticles have received a lot of technological scientific interest [17]. APT is an adamantane-

triazole hybrid compound with antibacterial and anti-inflammatory properties [18] and DFT approach is used to understand interaction metallic clusters and APT.

Methods

DFT method is used to find the interaction of APT with Ag/Au/Cu metal clusters (mC) with M06-2X/6-311++G(d,p) (drug)/LANL2DZ (Au Ag, Cu) method/basis set (Fig.1) [19-22]. The adsorption energy E = $E_{APT-mC} - E_{mC} - E_{APT}$, where E_{APT-mC}, E_{mC}, E_{AMT} are energies of APT-mC, mC and APT, respectively [23, 24]. The DOS plots were generated using the Gausssum suite of software [25].

Results And Discussion

Fig.2a and Fig.2b represent FMOS of mCs and APT and APT-mCs [26, 27]. For all mCs and APT, distributions of FMOs were over all atoms with interchange in polarity for all mC. Energy gap values are 2.0710, 1.0688, 0.0631 and 0.0332 eV for APT, APT-Ag, APT-Au and APT-Cu, respectively and show a decreasing nature for APT-mC system (table 1). Also the energy gaps APT-mC systems are less than that of pure mC systems. APT-Ag/Cu complexes had the highest and lowest values of Eg values. As a result, these two were found to be the least and the most electrically conductive, respectively. The value of Eg may be used to examine the mC's kinetic stability. The energy of HOMO and LUMO for APT are -7.0637 and -4.9927 eV with energy gap of 2.0710 eV. The bond distances from nanocages to S atom are: 2.7599, 2.6427 and 2.4995Å for APT-Ag, APT-Au and APT-Cu, respectively.

Table 1. Chemical descriptors of APT and APT-mC complexes (all parameters in eV)

System	E_{HOMO}	E_{LUMO}	Energy gap	Hardness	Chemical potential	Electrophilicity index
Ag	-6.2234	-4.1067	2.1167	1.0584	-5.1651	12.6029
Au	-4.0125	-3.2185	0.7940	0.3970	-3.6155	16.4633
Cu	-4.9657	-4.2169	0.7488	0.3744	-4.5913	28.1518
APT	-7.0637	-4.9927	2.0710	1.0355	-6.0282	17.5467
APT-Ag	-6.1143	-5.0455	1.0688	0.5344	-5.5799	29.1311
APT-Au	-4.4446	-4.3815	0.0631	0.0316	-4.4131	308.1489
APT-Cu	-4.9573	-4.9241	0.0332	0.0166	-4.9407	735.2565

The frequency calculations revealed that no imaginary vibrational frequency existed for APT-mC, indicating a true minimum. The reactive sites of APT and mC are attached to each other to form an

adsorption mechanism. The electronic and geometrical properties of mC clusters and complexes were investigated using dipole moment values (Table 2).

Table 2. NLO parameters

System	Dipole moment (Debye)	Polarizability (a.u.)	First order hyperpolarizability (a.u.)
APT	5.4810	338.6190	537.0370
APT-Ag	10.1119	646.4854	8515.3754
APT-Au	12.3244	613.8966	6860.2129
APT-Cu	7.9744	585.1252	7569.1595

After adsorption of the APT on isolated mC nanoclusters, considerable changes in the value of the dipole moment were observed. Because of their symmetry, the dipole moments of isolated mCs were zero, but increased after adsorption. The dipole moments are 10.1119 (APT-Ag), 12.3244 (APT-Au) and 7.9744 (APT-Cu) Debye while that of APT is 5.4810 Debye. The study of reactivity indices was crucial in determining the reactivity and stability of all, including APT, mC nanocages, and complexes. Hardness of APT was decreased during the adsorption onto nanoclusters, indicating that the reactivity of the resulting complex was higher than that of pure mC nanoclusters, implying that more APT molecules could be adsorbed on nanoclusters. When hardness was reduced, the softness increased indicating that reactivity of resulting complex increased after adsorption [28-30]. The electrophilicity index measures a fragment's ability to accept electrons [31]. Electrophilicity index increased in complexes with a propensity to accept electrons after APT adsorption on mCs relative to corresponding pristine systems. Also electrophilicity indices of the complexes are very much greater than that of APT (17.5467 eV) with highest value for APT-Cu (735.2565 eV) and lowest value for APT-Ag (29.1311 eV).

Adsorption of APT on mCs changes chemical potential (table 1) and the highest and least values of chemical potential shift belong to APT-Au (1.6151 eV) and APT-Ag (0.4483 eV). In APT, HOMO and LUMO are respectively over the triazole and phenyl ring attached to the triazole ring. HOMO of the complexed form of APT-mCs is over the mCs and on CS in the case of APT-Ag. LUMO are over the phenyl rings of APT-Ag, Au cluster and phenyl ring with piperazine of APT-Au and phenyl ring with piperazine for APT-Cu. Adsorption of APT on mCs resulted in certain changes in HOMO and LUMO energies. Eg of all APT-mC were decreased upon adsorption, resulting in an increase in conductivity which is useful for design of an electrochemical biosensor for APT.

Binding energies are: -56.46 kJ/mol (APT-Ag), -101.87 kJ/mol (APT-Au) and -57.14 kJ/mol (APT-Cu) and the large negative values implies chemisorption process. Fig.3 depicts the DOS spectra of mC-APT systems. The interaction of each nanocage with APT resulted in the appearance of new energy states at Fermi level, which resulted in decrease in Eg. Difference in Eg was calculated as 1.0022, 2.0079 and

2.0388 eV for APT-Ag, APT-Au and APT-Cu. Since energy gap depends electrical conductivity, it is expected that when the APT is complexed, the energy gap value will cause significant changes in electrical conductivity [32]. The effect on Eg and DOS is relatively small since APT-mC nanocages have higher adsorption energies. These findings suggest that while all mCs are good adsorbents for APT.

MEP is used for predicting desired binding sites and is primarily used in biological recognition [33]. MEP surfaces are shown in Fig.4 (mCs) and APT, APT-mCs (Fig.5). Different colours on the MEP surface were used to depict the sensitivity of electrostatic potential; intense red and dark blue colours represent high electronegative and electropositive potential. The polarity of the molecule increased as contrast between red and blue colour increased. Non-polarity was shown by lightening of colours or white shade. Sulfur atom and phenyl ring attached to the piperazine of APT were primarily responsible for the red and yellow areas. Higher electronegative and electropositive regions was over S, phenyl ring and N, H atoms, indicating sites for nucleophilic and electrophilic attacks. Ag and Cu clusters are electronegative for APT-mCs while Au cluster is electropositive for APT-Au system. Atoms of all APT(-mCs) follows the same behaviour as in the case of APT. The same nature is observed in the electrostatic potential contour in terms of closed and open contours. The APT's reactive spaces are useful for analzying APT-protein interactions [34]. The nucleophilic and electrophilic sections of APT and mCs are attached to each other to form adsorption mechanism. Polarizability of APT-mC complexes are very much greater than that of APT (Table 2). Hhyperpolarizability values show very large enhancement in APT-mC systems in comparison with that of APT [35].
Figs.6(a,b) shows Raman signals multiplication for multiple wavenumbers all APT-mC complexes. Mulliken charge analysis (table 3) show that all APT atom's charge changes due to the interactions with mCs. All the mC clusters are interacting thorough APT through the atoms, S, N atoms, C10, C12, C54 and C57 which get support from Mulliken charges. The charge of S1 is -0.011705 in APT changes to 0.061949, 0.116396 and 0.073528 in APT-Ag/Au/Cu systems due to interactions. Charges of N2, N3, N5/N4, N6 decreases/increases in APT-mCs. Charges of C10, C12, C54 and C57 also show variations due to complex formation. This suggests that a metal cluster-based sensor for APT detection could be made using SERS [36-38].

Table 3. Mulliken charges

Atom	APT	APT-Ag	APT-Au	APT-Cu
1 S	-0.011705	0.061949	0.116396	0.073528
2 N	-0.322449	-0.311613	-0.307394	-0.306592
3 N	-0.018049	-0.006233	-0.004732	-0.009833
4 N	-0.117169	-0.124982	-0.129625	-0.123643
5 N	-0.070156	-0.065452	-0.067432	-0.059924
6 N	-0.205608	-0.215614	-0.219362	-0.209281
7 C	-0.275276	-0.199362	-0.155315	-0.180413
8 C	0.054698	0.039467	0.039718	0.040654
9 C	0.444666	0.432657	0.438932	0.421318
10 C	-0.092876	-0.052451	-0.033813	-0.023438
12 C	0.024507	0.040634	0.045197	0.055470
14 C	0.004770	0.004814	0.006721	-0.002048
16 C	0.024051	0.022393	0.023753	0.017617
18 C	-0.089588	-0.079602	-0.090457	-0.084637
20 C	0.379162	0.369956	0.369392	0.372607
21 C	-0.104581	-0.100892	-0.100852	-0.099983
24 C	0.116084	0.116470	0.117463	0.116216
26 C	-0.070312	-0.067827	-0.067223	-0.068670
29 C	0.108838	0.109904	0.109810	0.109596
31 C	-0.105813	-0.102688	-0.103804	-0.101413
34 C	-0.067168	-0.063769	-0.062641	-0.063741
37 C	0.116268	0.119237	0.120901	0.117318
39 C	-0.069607	-0.066035	-0.065323	-0.066019
42 C	-0.103603	-0.089009	-0.087285	-0.079622
45 C	0.099063	0.116731	0.117729	0.115559
48 C	0.077181	0.097878	0.102721	0.100314
51 C	0.051241	0.052913	0.053076	0.057732
54 C	0.043212	0.068285	0.086800	0.069047

57 C	0.081205	0.132637	0.172110	0.112901
60 C	0.451486	0.460330	0.487068	0.464313
61 C	-0.163835	-0.161463	-0.173962	-0.156616
63 C	-0.000290	0.007665	0.018606	-0.001480
65 C	-0.038716	-0.033298	-0.024154	-0.031878
67 C	-0.009051	0.009980	0.046416	-0.008046
69 C	-0.140582	-0.121563	-0.116403	-0.131477

Conclusions

DFT studies of APT with various metal clusters of copper, gold and silver reported. The reactivity parametes were used to predict reactive sites in the molecule. Electronegative and electropositive regions were over S, phenyl ring and N, H atoms, indicating sites for nucleophilic and electrophilic attacks. Ag and Cu clusters are electronegative for APT-mCs while Au cluster is electropositive for APT-Au system. The APT-mC systems have very significant increase in NLO activity relative to APT. Raman signals in mC complexes show enhancement. Overall results proposed that APT-Au has better adsorption energy.

Declarations

Funding: This research was funded by the Deanship of Scientific Research at Princess Nourah bint Abdulrahman University through the Fast-track Research Funding Program

Conflict of interest: The authors declare no competing interests.

Data availability: All data are available on request to the corresponding author

Code availability: N/A

Author's contributions: Conceptualization, Y.Sheena Mary; Methodology, Y.Shyma Mary; Writing original draft, Jamelah S.Al-Otaibi, Y.Sheena Mary; Writing-review and editing, Jamelah S.Al-Otaibi, Y.Sheena Mary, Y.Shyma Mary

Ethics approval

The manuscript is prepared in compliance with the Ethics in Publishing Policy as described in the Guide for Authors

Consent to participate

The manuscript is approved by all authors for publication

Consent for publication

The consent for publication was obtained from all participants

References

[1] S.A.El-Sebaey, Recent Advances in1,2,4-triazole scaffolds as antiviral agents, ChemistrySelect 5 (2020) 11654-11680. https://doi.org/10.1002/slct.202002830

[2] W.Furuyama, A.Marzi, Ebola Virus: Pathogenesis and countermeasure development, Annu. Rev. Virol. 6 (2019) 435-458. https://doi.org/10.1146/annurev-viorology-092818-015708

[3] D.Musso, A.I.Ko, D.Baud, Zika virus infection-After the pandemic, N. Engl. J. Med. 381 (2019) 1444-1457. https://doi.org/10.1056/NEJMra1808246

[4] R.Kharb, M.S.Yar, P.C.Sharma, Recent advances and future perspectives of triazole analogs as promising antiviral agents, Mini-Rev. Med. Chem. 11 (2010) 84-96. https://doi.org/10.2174/13895571193564051

[5] G.Khan, S.Sreenivasa, S.Govindaiah, V.Chandramohan, P.R.Shetty, Synthesis, biological screening, in silico study and fingerprint applications of novel 1,2,4-triazole derivatives, J. Heterocycl. Chem. 57 (2020) 2010-2023. https://doi.org/10.1002/jhet.3929

[6] V.H.Pam, T.P.D.Phan, D.C.Phan, B.D.Vu, Synthesis and bioactivity of thiosemicarbazones containing adamantane skeletons, Molecules 25 (2020) 324. https://doi.org/10.3390/molecles25020324

[7] I.Stankova, K.Chuchkov, R.chayrov, L.Mukova, A.Galabov, D.Marinkova, D.Danalev, Adamantane derivatives containing thiazole moiety: synthesis, antiviral and antibacterial activity, Int.J. Pept. Res. Ther. 26 (2020) 1781-1787. https://doi.org/10.1007/s10989-019-09983-4

[8] X.Zhu, J.Sun,S.Wang, W.Bu, M.Yao, K.Gao,Y.Song, J.Zhao, C.Lu, E.Zhang, Synthesis, crystal structure, superoxide scavenging activity, anticancer and docking studies of novel adamantly nitroxide derivatives, J. Mol. Struct. 1108 (2016) 611-617. https://doi.org/10.1016/j.molstruc.2015.12.048

[9] V.Burmistrov, C.Morisseau, D.Karlov, D.Pitushkin, A.Vernigora, E.Rasskazova, G.M.Butov, B.D.Hammock, Bioisosteric substitution of adamantane with bicyclic lipophilic groups improves water solubility of human soluble epoxide hydrolase inhibitors, Bioorg. Med. Chem. Lett. 30 (2020) 127430. https://doi.org/10.1016/j.bmcl.2020.127430

[10] V.M.Dembitsky, T.A.Gloriozova, V.V.Poroikov, Pharmacological profile of natural and synthetic compounds with adamantane-based scaffolds as potential agents for the treatment of

neurodegenerative diseases, Biochemical and Biophysical Research Communications 529 (2020) 1225-1241. https://doi.org/10.1016/j.bbrc.2020.06.123

[11] P.Horcajada, T.Chalati, C.Serre, B.Gillet, C.Sebrie, T.Baati, J.F.Eubank, D.Heurtaux, P.Clayette, C.Kreuz, J.S.Chang, Y.K.Hwang, V.Marsaud, P.N.Bories, L.Cynober, S.Gil, G.Ferey, P.Couvreur, R.Gref, Porous metal organic frame work nanoscale carriers as a potential platform for drug delivery and imaging, Nat. Mater. 9 (2010) 172-178. https://doi.org/10.1038/nmat2608

[12] X.M.Kang, H.S.Hu, Z.L.Wu, J.Q.Wang, P.Cheng, J.Li, B.Zhao, An ultrastable matryoshka [Hf13] nanocluster as a luminescent sensor for concentrated alkali and acid, Angew. Chem. Int. Ed. 58 (2019) 16610-16616. https://doi.org/10.1002/anie.201907557

[13] T.L.Silbaugh, P.Devlaminck, J.A.Sofranko, M.A.Barteau, Selective oxidation of ethanol over Ag, Cu and Au nanoparticles supported on Li2O/γ-Al2O3, J. Catal. 364 (2018) 40-47. https://doi.org/10.1016/j.cat.2018.05.011

[14] R.-Y.Wang, J.-X.Wang , J.Jia, H.-S.Wu , The growth pattern and electronic structures of Cun(n=1-14) clusters on rutile TiO2(1 1 0) surface, Applied Surface Science 536 (2021) 147793. https://doi.org/10.1016/j.apsusc.2020.147793

[15] S.Pramanik, S.Chatterjee, A.Saha, P.S.Devi, G.S.Kumar, Unravelling the interaction of silver nanoparticles with mammalian and bacterial DNA, J. Phys. Chem. B 120 (2016) 5313-5324. https://doi.org/10.1021/acs.jpcb.6b01586

[16] M.C.Shukla, M.Dubey, E.Zakar, J.Leszczynski, DFT investigation of the interaction of gold nanoclusters with nucleic acid base guanine and the Watson-Crick guanine-cytosince base pair, J. Phys. Chem. C 113 (2009) 3960-3966. https://doi.org/10.1021/jp808622y

[17] L.F.de Freitas, G.H.C.Varca, J.G.dos Santos Batista, A.B.Lugao, An overview of the synthesis of gold nanoparticles using radiation technologies, Nanomaterials 8 (2018) 939. https://doi.org/10.3390/nano8110939

[18] E.S. Al-Abdullah, H.H. Asiri, S. Lahsasni, E.E. Habib, T.M. Ibrahim, A.A. El-Emam, Synthesis, antimicrobial, and anti-inflammatory activity, of novel *S*-substituted and *N*-substituted 5-(1-adamantyl)-1,2,4-triazole-3-thiols, Drug Des. Dev. Ther. 8 (2014) 505-518. https://doi.org/10.2147/DDDT.S62465

[19] Gaussian 09, Revision C.01, M.J. Frisch, G.W. Trucks, H.B. Schlegel, G.E. Scuseria, M.A. Robb, J.R. Cheeseman, G. Scalmani, V. Barone, B. Mennucci, G.A. Petersson, H. Nakatsuji, M. Caricato, X. Li, H.P. Hratchian, A.F. Izmaylov, J. Bloino, G. Zheng, J.L. Sonneberg, M. Hada, M. Ehara, K. Toyota, R. Fukuda, J. Hasegawa, M. Ishida, T. Nakajima, Y. Honda, O. Kitao, H. Nakai, T. Vreven, J.A. Montgomery, J.E. Peralta, F. Ogliaro, M. Bearpark, J.J. Heyd, E. Brothers, K.N. Kudin, V.N. Staroverov, T. Keith, R. Kobayashi, J. Normand, K. Raghavachari, A. Rendell, J.C. Knox, J.B. Cross, V. Bakken, C. Adamo, J. Jaramillo, R.

Gomperts, R.E. Stratmann, O. Yazyev, A.J. Austin, R. Cammi, C. Pomelli, J.W. Ochterski, R.L. Martin, K. Morokuma, V.G. Zakrzewski, G.A.Voth, P. Salvador, J.J. Dannenberg, S. Dapprich, A.D. Daniels, O. Farkas, J.B. Foresman, J.V. Ortiz, J. Cioslowski, D.J. Fox, Gaussian Inc., Wallingford CT, 2010.

[20] J.B. Foresman, A Guide to Using Gaussian, Pittsburg, PA, in E: Frisch (Ed.), Exploring Chemistry with Electronic Structure Methods, 1996.

[21] R. Dennington, T. Keith, J. Millam, Gaussview, Version 5, Semichem Inc., Shawnee Missions KS, 2009.

[22] Z.Ullah, R.Thomas, Markovnikov versus anti-Markovnikov addition and C-H activation: pd-Cu synergistic catalysis, Applied Organometallic Chemistry 35 (2021) e6077. https://doi.org/10.1002/aoc.6077

[23] A.H.Almuqrin, J.S.Al-Otaibi, Y.S.Mary, Y.S.Mary, R.Thomas, Structural study of letrozole and metronidazole and formation of self-assembly with graphene and fullerene with the enhancement of physical, chemical and biological activities. Journal of Biomolecular Structure and Dynamics (2020). https://doi.org/10.1080/07391102.2020.1790420

[24] J.S.Al-Otaibi, Y.S.Mary, R.Thomas, S.Kaya, Detailed electronic structure, physico-chemical properties, excited state properties, virtual bioactivity screening and SERS analysis of three guanine based antiviral drugs, valacyclovir HCl hydrate, acyclovir and ganciclovir. Polycyclic Aromatic Compounds (2020). https://doi.org/10.1080/10406638.2020.1773876

[25] N.M.O'boyle, A.L.Tenderholt, K.M.Langner, Cclib: a library for package independent computational chemistry algorithms. Journal of Computational Chemistry 29 (2008) 839-845. https://doi.org/10.1002/jcc.20823

[26] A.M.Teale, F.De Proft, D.J.Tozer, Orbital energies and negative electron affinities from density functional theory: Insight from integer discontinuity, J. Chem. Phys. 129 (2008) 044110. https://doi.org/10.1063/1.2961035

[27] K.Burke, L.O.Wagner, DFT in a nutshell, Int. J. Quantum Chem. 113 (2013) 96-101. https://doi.org/10.1002/qua.24259

[28] R.G.Pearson, Absolute electronegativity and hardness: Application to inorganic chemistry, Inorg. Chem. 27 (1988) 734-740. https://doi.org/10.1021/ic00277a030

[29] H.Xu, D.C.Xu, Y.Wang, Natural indices for the chemical hardness/softness of metal cations and ligands, ACS Omega, 10 (2017) 7185-7193. https://doi.org/10.1021/acsomega.7b01039

[30] R.K.Roy, S.Krishnamurti, P.Geerlings, S.Pal, Local softness and hardness based reactivity descriptors for predicting intra- and intermolecular reactivity sequences: Carbonyl compounds, J. Phys. Chem. A 102 (1998) 3746-3755. https://doi.org/10.1021/jp973450v

[31] A.Nicolai, B.G.Sumpter, V.Meunier, Tunable water desalination across graphene oxide framework membranes. Phys. Chem. Chem. Phys. 16 (2014) 8646-8654. https://doi.org/10.1039/C4CP01051E

[32] S. Li, Semiconductor Physical Electronics, second ed. Springer, Berlin, 2006.

[33] Y.S.Mary, C.Y.Panicker, M.Sapnakumari, B.Narayana, B.K.Sarojini, A.A.Al-Saadi, C.Van Alsenoy, J.A.War, H.K.Fun, Molecular structure, FT-IR, Vibrational assignments, HOMO-LUMO analysis and molecular docking study of 1-[5-(4-Bromophenyl)-3-(4-fluorophenyl)-4,5-dihydro-1*H*-pyrazol-1-yl]ethanone. Spectrochim Acta 136 (2015) 473-482. https://doi.org/10.1016/j.saa.2014.09.060

[34] B.Sureshkumar, Y.S. Mary, C.Y.Panicker, S.Suma, S.Armakovic, S.J.Armakovic, C.Van Alsenoy, B.Narayna, Quinoline derivatives as possible lead compounds for anti-malarial drugs: Spectroscopic, DFT and MD study Arabian Journal of Chemistry 13 (2020) 632-
648. https://doi.org/10.1016/j.arabjc.2017.07.006

[35] Y.S.Mary, H.T.Varghese, C.Y.Panicker, M.Girisha, B.K,Sagar, H.S.Yathirajan, A.A.Al-Saadi, C.Van Alsenoy, Vibrational spectra, HOMO, LUMO, NBO, MEP analysis and molecular docking study of 2,2-diphenyl-4-(piperidin-1-yl)butanamide, Spectrochim. Acta 150 (2015) 543-556.
https://doi.org/10.1016/j.saa.2015.05.090

[36] J.S.Al-Otaibi, Detailed quantum mechanical studies on bioactive benzodiazepine derivatives and their adsorption over graphene sheets. Spectrochim Acta 235 (2020)
118333. https://doi.org/10.1016/j.saa.2020.118333

[37] J.S.Al-Otaibi, A.H.Almuqrin, Y.S.Mary, Y.S.Mary, Comprehensive quantum mechanical studies on three bioactive anastrozole based triazole analogues and their SERS active graphene complex. Journal of Molecular Structure 1217 (2020) 128388. https://doi.org/10.1016/j.molstruc.2020.128388

[38] U.Bhattacharyya, T.Pooventhiran, R.Thomas, Adsorption of the drug bempedoic acid over different 2D/3D nanosurfaces and enhancement of Raman activity enabling ulstrasensitive detection: First principle analysis, Spectrochim. Acta 254 (2021) 119630. https://doi.org/10.1016/j.saa.2021.119630

Figures

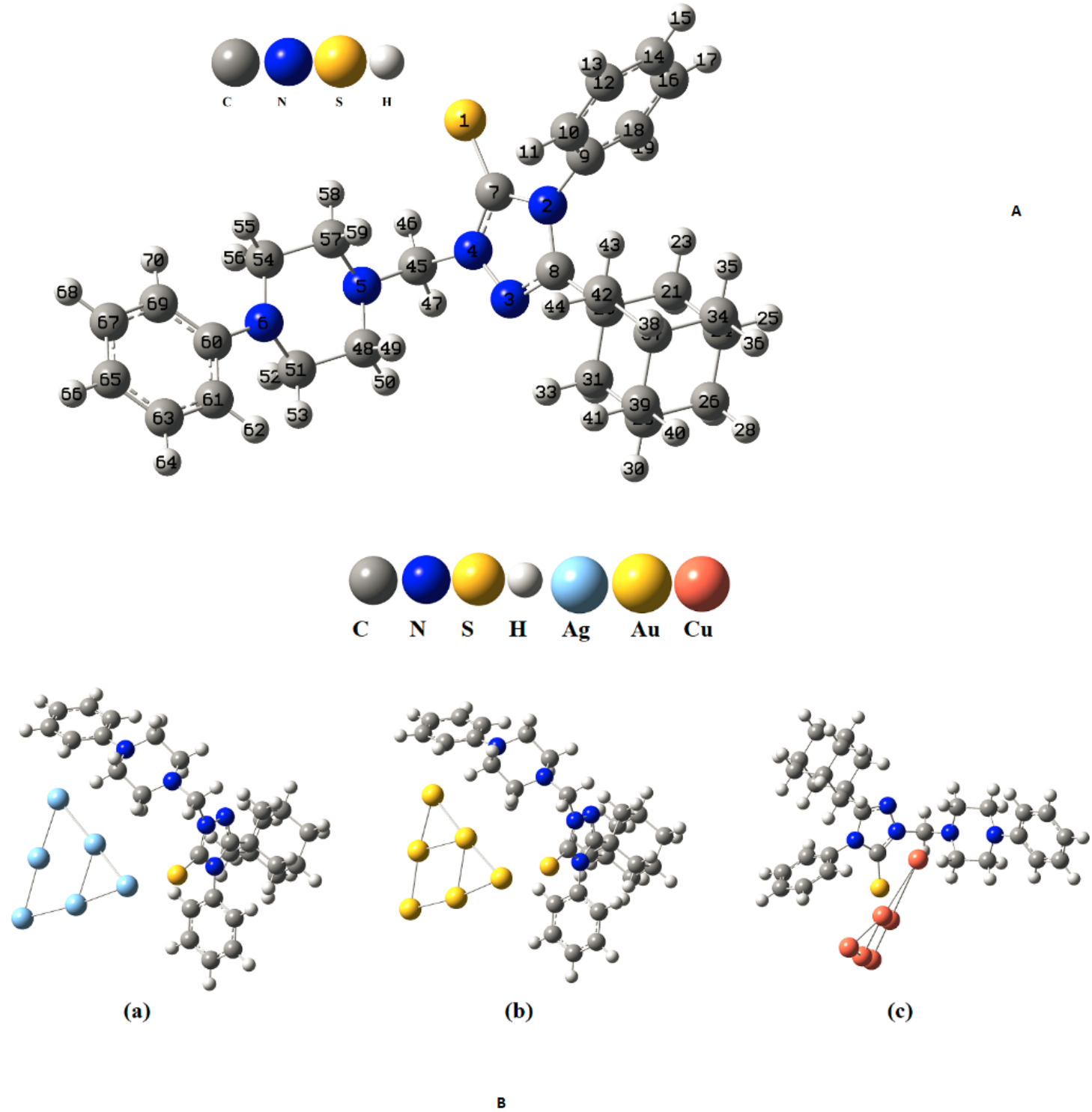

Figure 1

a. Optimized geometry of APT b. Optimized geometries of (a) APT-Ag (b) APT-Au (c) APT-Cu

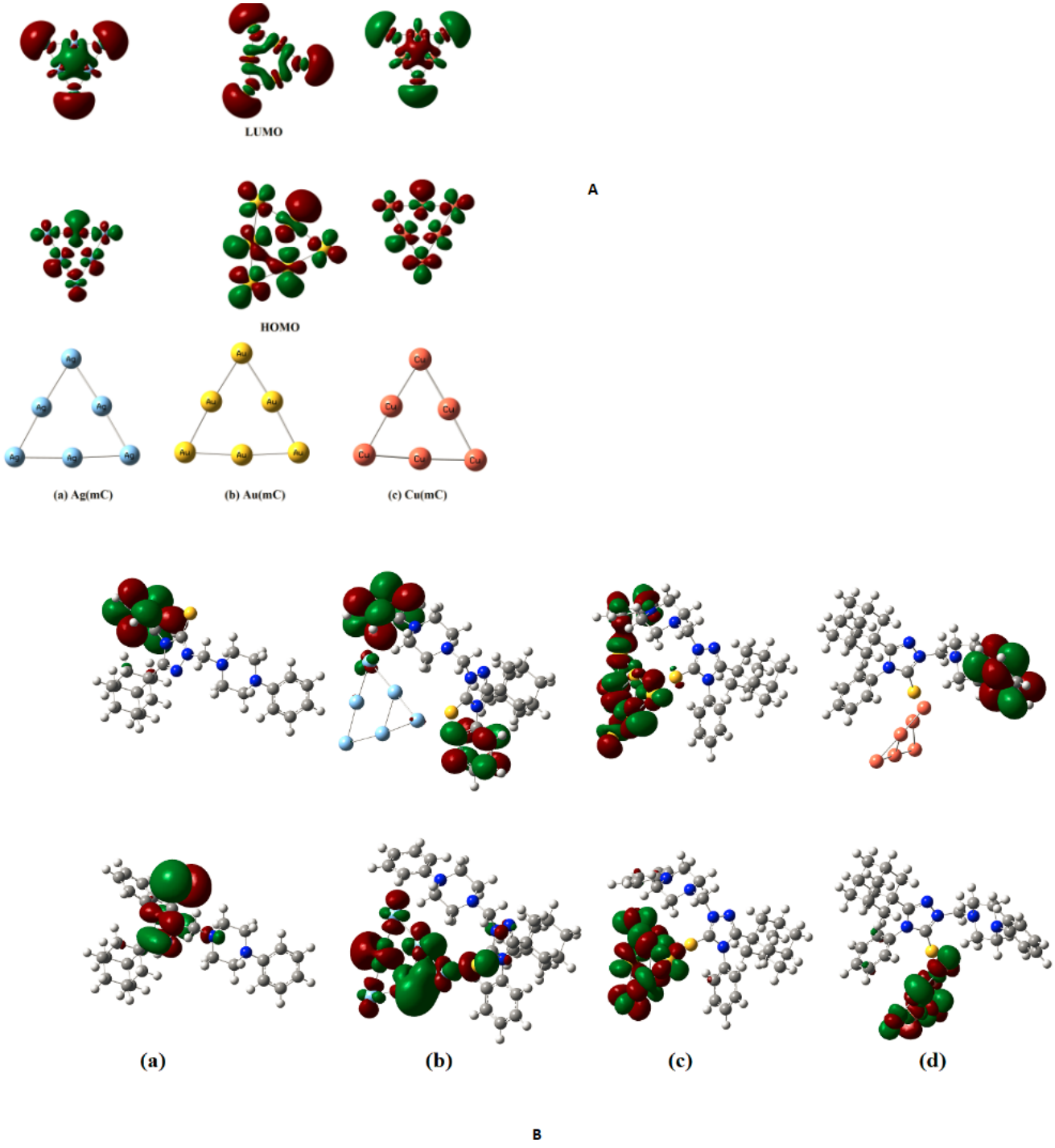

Figure 2

a. HOMO-LUMO plots of metal clusters (a) Ag (b) Au (c) Cu b. HOMO-LUMO plots of (a) APT (b) APT-Ag (c) APT-Au (d) APT-Cu

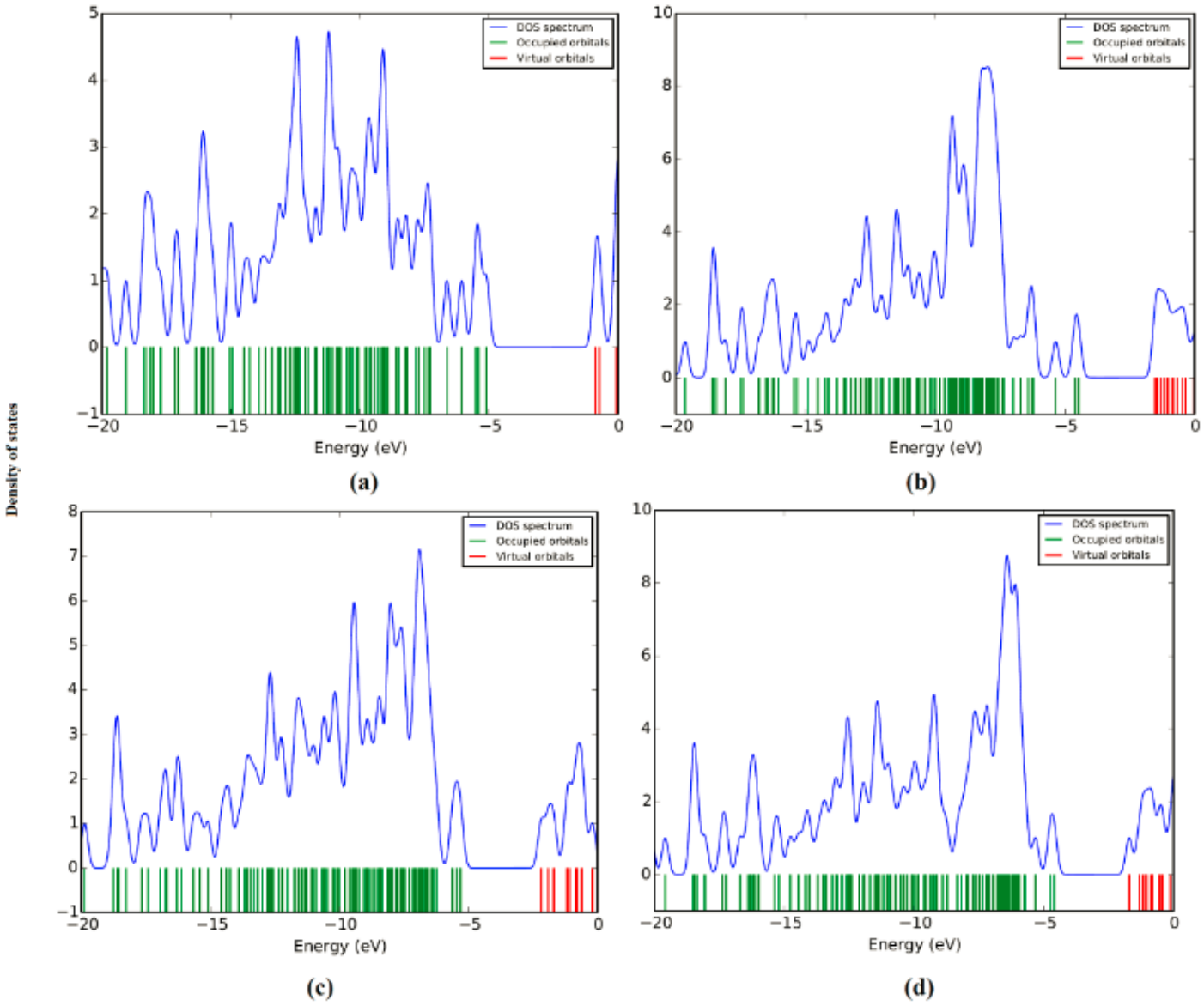

Figure 3

DOS spectra of (a) APT (b) APT-Ag (c) APT-Au (d) APT-Cu

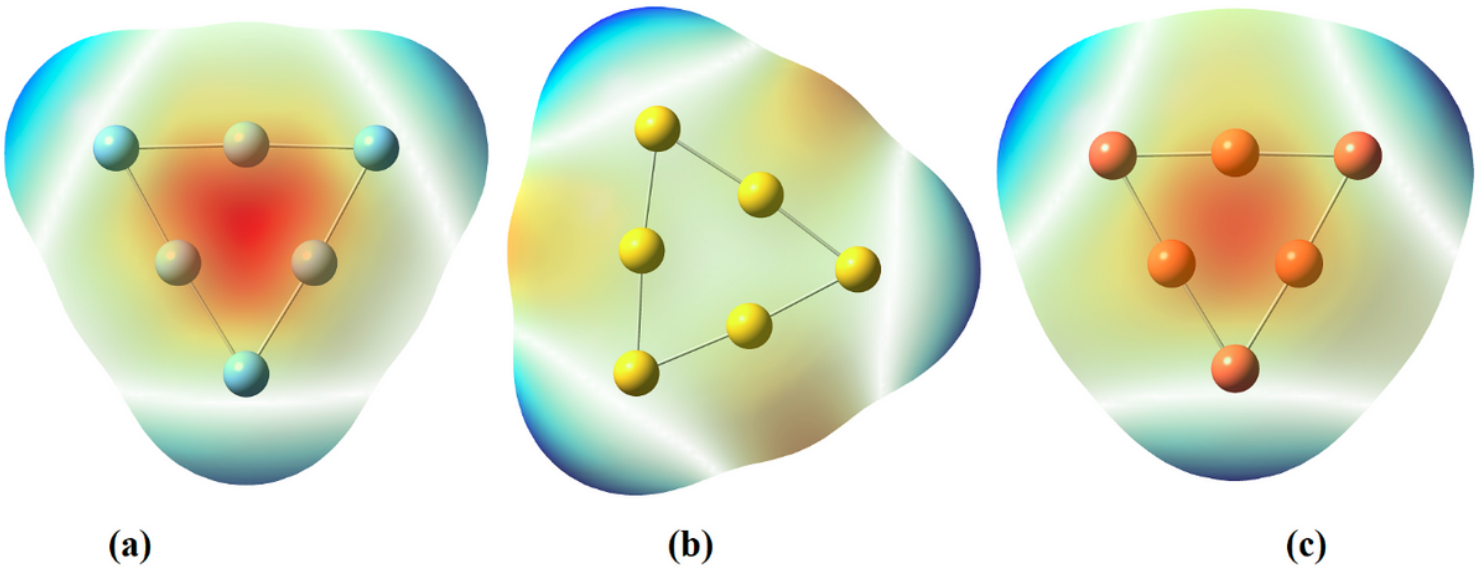

Figure 4

MEP plots of metal clusters (a) Ag (b) Au (c) Cu

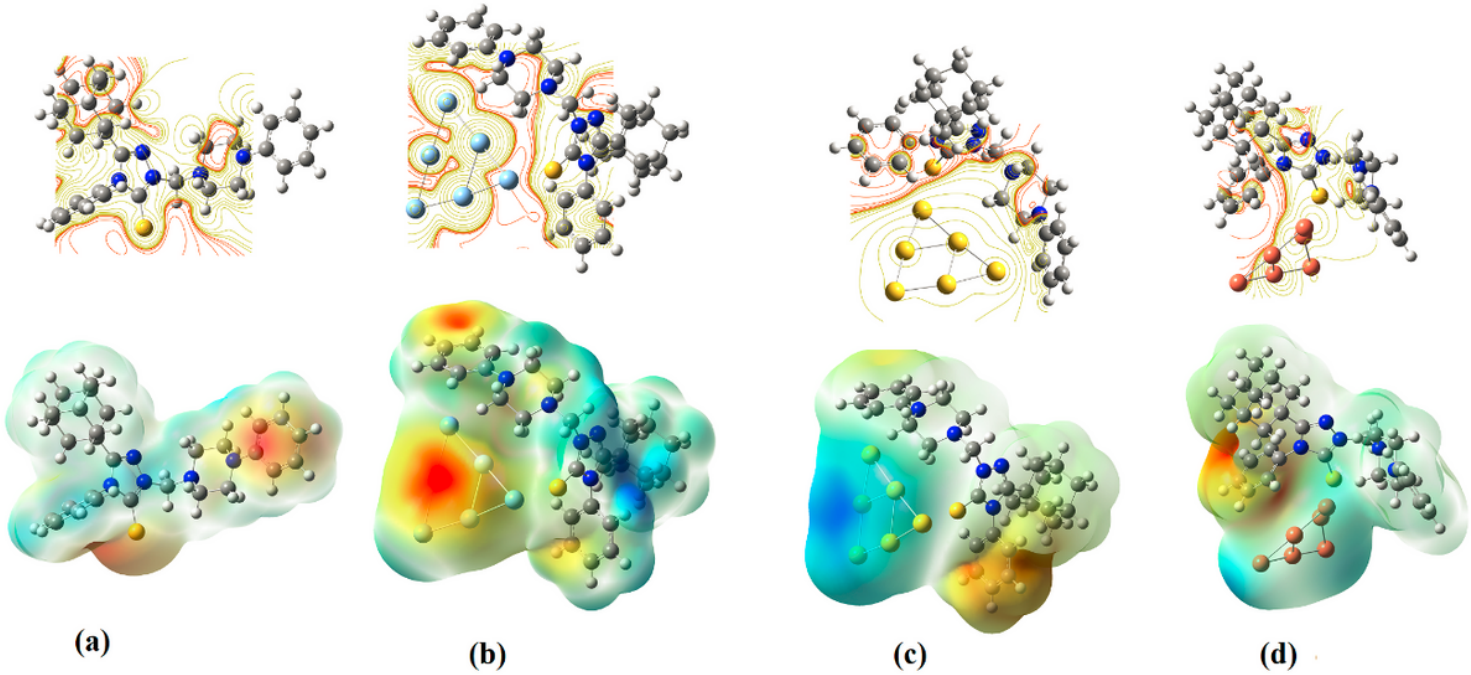

Figure 5

MEP plots of (a) APT (b) APT-Ag (c) APT-Au (d) APT-Cu

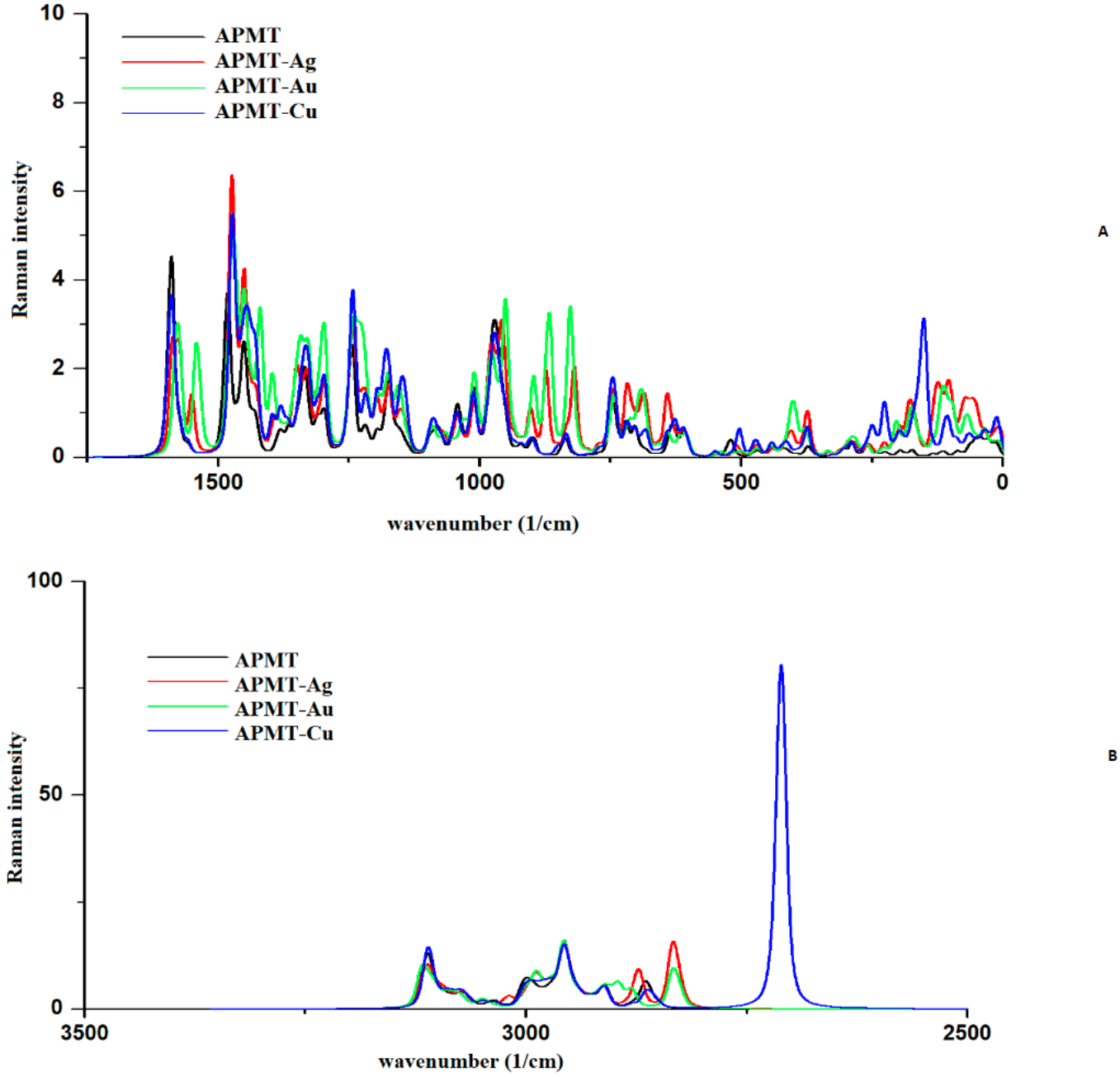

Figure 6

a. Theoretical Raman spectra of (a) APT (b) APT-Ag (c) APT-Au (d) APT-Cu in the range 1750-0 cm-1 b. Theoretical Raman spectra of (a) APT (b) APT-Ag (c) APT-Au (d) APT-Cu in the range 350-2500 cm-1

Supplementary Files

This is a list of supplementary files associated with this preprint. Click to download.

- graphicalabstract.docx